

The Small Scatter in BH-Host Correlations & The Case for Self-Regulated BH Growth

Philip F. Hopkins^{1*}, Norman Murray^{2,3}, & Todd A. Thompson^{4,5}

¹Department of Astronomy, University of California Berkeley, Berkeley, CA 94720

²Canadian Institute for Theoretical Astrophysics, 60 St. George Street, University of Toronto, ON M5S 3H8, Canada

³Canada Research Chair in Astrophysics

⁴Department of Astronomy, The Ohio State University, 140 W. 18th Ave., Columbus, OH 43210

⁵Center for Cosmology & Astro-Particle Physics, The Ohio State University, 191 W. Woodruff Ave., Columbus, OH 43210

Submitted to MNRAS, March 17, 2009

ABSTRACT

Supermassive black holes (BHs) obey tight scaling relations between their mass and their host galaxy properties such as total stellar mass, velocity dispersion, and potential well depth. This has led to the development of self-regulated models for BH growth, in which feedback from the central BH halts its own growth upon reaching a critical threshold. However, models have also been proposed in which feedback plays no role: so long as a fixed fraction of the host gas supply is accreted, relations like those observed can be reproduced. Here, we argue that the *scatter* in the observed BH-host correlations presents a demanding constraint on any model for these correlations, and that it favors self-regulated models of BH growth. We show that the scatter in the stellar mass fraction within a radius R in observed ellipticals and spheroids increases strongly at small R . At fixed total stellar mass (or host velocity dispersion), on very small scales near the BH radius of influence, there is an order-of-magnitude scatter in the amount of gas that must have entered and formed stars. In short, the BH appears to “know more” about the global host galaxy potential on large scales than the stars and gas supply on small scales. This is predicted in self-regulated models; however, models where there is no feedback would generically predict order-of-magnitude scatter in the BH-host correlations. Likewise, models in which the BH feedback in the “bright” mode does not regulate the growth of the BH itself, but sets the stellar mass of the galaxy by inducing star formation or blowing out a mass in gas much larger than the galaxy stellar mass, are difficult to reconcile with the scatter on small scales.

Key words: galaxies: formation — galaxies: evolution — galaxies: active — quasars: general — cosmology: theory

1 INTRODUCTION

The tight empirical correlations between the masses of supermassive black holes (BHs) and the velocity dispersion, masses, and binding energy or potential well depth of their hosts demonstrates a fundamental link between the growth of BHs and galaxy formation (e.g., Magorrian et al. 1998; Ferrarese & Merritt 2000; Gebhardt et al. 2000; Aller & Richstone 2007; Hopkins et al. 2007b). Understanding the physical origin and consequences of these correlations is critical for informing models of the co-formation of BHs and bulges, as well as theories which relate the evolution and statistics of BH formation and quasar activity to the remnant spheroid population. Likewise, the interpretation of observations tracing the buildup of spheroid populations and associations

between spheroids in formation, mergers, and quasar hosts depends on understanding the evolution of the BH-host correlations.

Although the characteristic spatial and mass scales of the BH and tightly correlated host properties are wildly different, their characteristic energy and momentum scales are the same. That is, a few percent of the radiated luminosity or momentum from the BH growth is comparable to the binding energy/momentum of the galactic gas supply. Motivated by this comparison, attempts to explain these correlations have led to the development of a class of self-regulating feedback models, which argue that the energy or momentum released from an accreting supermassive black hole, even if only a small fraction couples to the surrounding ISM, is sufficient to halt further accretion onto the black hole and drive away gas, self-regulating growth by shutting off the quasar and potentially quenching star formation in the host. (see, e.g., Ciotti & Ostriker 1997, 2001; Silk & Rees 1998; Murray et al.

* E-mail:phopkins@astro.berkeley.edu

2005; Di Matteo et al. 2005; Sazonov et al. 2005; Hopkins et al. 2005, 2006a,b; Springel et al. 2005). In these models, star formation and inflows proceed rapidly before the final stages of BH growth, so that the BH grows in a relatively fixed background potential, which sets the critical BH accretion rate at which the BH halts its own subsequent growth.¹ Implicit in these models, the idea that the BH growth is fueling in sudden, violent events (mergers) that lead to strong bulge and BH growth, links the formation of both (it is less clear whether or not such models could succeed if growth occurred more slowly, in low accretion rate states, where there might be little bulge formation and/or feedback).

The gas mass blown out by the BH may be an order of magnitude larger than the BH mass itself, but is still a small fraction of the total galaxy mass; it is the mass “left over” from a central starburst. This picture is in part supported by observations of quasar-driven outflows that find evidence for momentum and energy content comparable to that required by models (see, e.g., Tremonti et al. 2007; Reuland et al. 2007; Arav et al. 2007; Nesvadba et al. 2006; Prochaska & Hennawi 2009), but remains highly uncertain.

In contrast, a separate class of models have been proposed to explain the BH-host correlations (or a subset) without feedback or self-regulation. An example is this: because the observed correlation between BH mass and host bulge stellar mass is approximately linear ($M_{\text{BH}} \propto M_{\text{bulge}}$), if a fixed average fraction ($\sim 10^{-3}$) of the galactic baryon supply is able to reach the center and fuel the BH, this particular observed correlation can be explained. The efficiency of angular momentum transport as well as the competition between gas accretion and star formation, explains a small mean constant of proportionality (Burkert & Silk 2001; Escala 2007; Li et al. 2007). Alternatively, stellar capture rates by the central BH based on the average central stellar density profile also lead to an expectation for the average BH accretion rate (see, e.g., Miralda-Escudé & Kollmeier 2005).

Although it is possible for these models to explain the mean correlation between BH mass and host mass, a more stringent constraint comes from the surprisingly small observed scatter in that correlation, which observations suggest is at most $\sim 0.25 - 0.3$ dex (in terms of the constrained intrinsic scatter in M_{BH} versus M_{bulge} , σ , or host potential depth/binding energy; see Tremaine et al. 2002; Marconi & Hunt 2003; Häring & Rix 2004; Graham & Driver 2007; Hopkins et al. 2007b; Aller & Richstone 2007). It has already been argued that this scatter (compared to that in other correlations) suggests that it must be galaxy properties, rather than e.g. the properties of the larger dark matter halo, that are important for whatever sets the BH mass (Wyithe & Loeb 2005). In addition, the small scatter puts strong constraints on models where the mean relation evolves very strongly with redshift (Robertson et al. 2006), although more moderate evolution as has been suggested from some observations is more easily reconciled with the low-redshift observations (see e.g. Peng et al. 2006; Hopkins et al. 2006c; Salvander et al. 2007; Woo et al. 2006).

But the observed scatter also places strong constraints on whether or not some non-feedback mechanisms could be responsible for the observed correlations. It is not hard to imagine, after all, that — on average — $\sim 10^{-3}$ of the galactic gas supply in most galaxies loses sufficient angular momentum to reach the BH radius

of influence and ultimately accrete. What is hard to imagine is that it would *always* be this same fraction to within better than a factor ~ 2 , regardless of the huge diversity in observed galaxy gas fractions, gas and stellar mass density profiles, and kinematic states. On large scales where viscous forces are sub-dominant and gas dynamics are largely gravitational, simulations of a galaxy merger or interaction suggest that even small changes to orbital parameters (say, changing relative disk inclinations, which are expected to vary widely, by a couple tens of degrees) lead to very large (nearly order-of-magnitude) changes in the amount of gas that loses such a large fraction of the angular momentum; from the galactic perspective, $\sim 10^{-3}$ and $\sim 10^{-2}$ are both small, gravitationally negligible gas masses, so why should one be “picked out” so narrowly?

At the opposite extreme, some models have proposed that feedback is so strong that the BH directly determines the stellar mass of the galaxy on a short timescale, as opposed to the feedback models already mentioned in which the BH feedback primarily regulates its own growth. Such a scenario implicitly requires that the BH form in the background of a gas-dominated galaxy. The BH feedback is then assumed to either blow out all but the “desired” mass, which will become the final stellar mass appropriate for the observed correlations,² or to directly induce star formation, causing the formation of the appropriate mass in stars (see e.g. King 2003, 2005; Granato et al. 2004; Silk 2005; Begelman & Nath 2005). In these models, then, the BH mass is not a function of galaxy mass; rather, galaxy mass is a function of BH mass. As such, the scatter in such an inverse correlation is a strong constraint on these models. Moreover, because the galaxy mass formed at some distance from the BH depends explicitly on the BH mass, the simple expectation is that galaxies of a given BH mass should have similar stellar mass profiles near the BH where the galaxy can most directly “feel” the BH mass, but with increasing scatter at larger radii, where various effects will introduce scatter in “how much” of the BH feedback successfully affects gas at that initial radius.

In this paper, we use observed galaxy stellar mass profiles and observations of gas masses, together with simulations of gas inflows in galaxy interactions and mergers, to constrain the origin of the M_{BH} -host galaxy correlations. We show that both observed galaxies and simulations exhibit a large scatter in the amount of gas that loses sufficient angular momentum to reach very small radii. Despite this order-of-magnitude scatter, the BH preserves (or sets) its mass such that it is correlated with the host on much larger scales to better than a factor of ~ 2 . The fact that the total stellar mass on small scales has much larger scatter than on large scales is hard to reconcile with most existing models in which the BH is simply sensitive to the *local* mass supply. Indeed, this suggests that some process such as feedback should be present in order for the BH to be sensitive to *global* quantities such as the total mass of the galaxy (or total binding energy/central gas potential). The systematics in the radial distribution of scatter in the stellar mass also present a strong constraint on the most extreme feedback models, in which galaxy mass is set by BH mass, because these models must explain why the stellar mass at small radii is a less accurate tracer of the BH mass than at large radius.

¹ Even if the trigger for rapid BH growth is a galaxy merger, the background potential at the galactic center relaxes sufficiently quickly that it is effectively fixed at the growth stage of interest (see, e.g., Hopkins et al. 2007a, 2008b; Younger et al. 2008).

² This is distinct from more common models of “radio” or “quiescent”-mode AGN feedback, in which AGN feedback regulates the final stellar mass of the galaxy over long timescales by heating gas in a massive group or cluster halo (see e.g. Croton et al. 2006).

2 OBSERVATIONS: THE SCATTER IN THE ENCLOSED STELLAR MASS FRACTION IN ELLIPTICAL GALAXIES

If the central BH mass were set by a fixed small fraction of the host mass reaching the central region, or if BH growth was determined by the central gas supply, we should expect that gas supply to be similarly well-correlated with the galaxy mass as is the BH mass. Although it is not possible to directly measure the total gas content that reached a given radius during BH growth, we can estimate this quantity and set a strict lower limit on it by measuring the *stellar* mass inside a given radius in local spheroids. To lowest order, this will simply trace the total gas content that reached that radial scale. We discuss possible corrections to this below, but note that, strictly this sets a lower limit to the gas content that has entered a given galactic radius.

Given a galaxy radial stellar surface density profile of the form $\Sigma(R)$, we integrate to determine the mass within R , $M(< R)$. Since we are interested in comparing with BH mass, which follows a linear relationship with total galaxy stellar mass ($M_{\text{BH}}/M_{\text{tot}} \equiv \mu_{\text{BH}} \approx 0.0012$ is assumed for all galaxies in the sample; see Häring & Rix 2004), we divide out the total mass and obtain the quantity of interest, the mass fraction within R , $f(< R) \equiv M(< R)/M_{\text{tot}} \approx L(< R)/L_{\text{tot}}$ (the last equality being for the observed surface brightness profile in any band where the mass-to-light ratio is a weak function of radius). Specifically

$$f(< R) = \frac{M(< R)}{M_{\text{tot}}} \equiv \frac{\int_0^R \Sigma(R') 2\pi R' dR'}{\int_0^\infty \Sigma(R') 2\pi R' dR'}. \quad (1)$$

The quantity $f(< R)$ is at fixed *physical* size: systems with different effective radii will have significantly different $f(< R)$ at the same R . Because the effective radius R_e varies significantly as a function of total stellar mass, this would alone imply (even if galaxy profile shapes were identical) a very large variation in a population of galaxies in $f(< R)$ at small R . Even at fixed stellar mass, the factor $\sim 2 - 3$ scatter in $R_e(M_{\text{tot}})$ implies more than an order-of-magnitude scatter in $f(< R)$ at small R if all galaxies have identical $r^{1/4}$ -law de Vaucouleurs (1948) profiles. Moreover, if the mass of the BH is a constant fraction of the mass of the host, then the BH radius of influence — the radius that should matter for the gas supply available for accretion — is a constant fraction of R_e (since this radius is where the potential contributed by the BH and galaxy stellar mass are similar, i.e. $GM_{\text{BH}}/R_{\text{BH}} \approx GM_{\text{tot}}/R_e$, hence $R_{\text{BH}} \approx \mu_{\text{BH}} R_e$). It is therefore more appropriate (and allows us to compare all objects on equal footing) to consider the mass fraction within a fraction of the effective radius, $f(< R/R_e)$ (equivalently, to refer to all radii in units of the effective radius of the galaxy, rather than fixed physical units).³ In short, for any fraction of the effective radius (or multiple of the BH radius of influence), we determine the fraction of the galactic gas supply that was available to turn into stars $f(< R/R_e)$ by measuring the stellar mass fraction inside that R/R_e .

The quantity of interest is, however, not the median value of $f(< R/R_e)$ (that is only a restatement of the typical profile shape of ellipticals), but how much *scatter* there is in $f(< R/R_e)$ at R/R_e . Specifically, we consider a subsample of galaxies (usually at fixed stellar mass, to further marginalize over possible systematic differences, although we find this makes little difference), and determine $f(< R/R_e)$ by integrating the surface brightness measurements available, from the minimum resolution elements out to R_e .

³ By definition the mass fraction inside R_e , $f(< R/R_e = 1) = 1/2$.

For all the objects we consider, measurements extend to radii very much larger than R_e .

We then determine the scatter in $\log[f(< R/R_e)]$, $\sigma[M(< R)/M_{\text{tot}}]$, in that sample at each R/R_e , either by assuming the distribution is lognormal and fitting it as such, or by taking the IPV value to reduce bias from outliers or skewness. We find it makes no difference. In terms of the simple dispersion (rather than a more complex fitted IPV value) this is

$$\sigma[f] = \sqrt{\frac{1}{N} \sum_i^N (\log f_i - \langle \log f \rangle)^2}, \quad (2)$$

with $f \equiv f(< R/R_e)$ evaluated for all N galaxies at the same R/R_e , and $\langle \log f \rangle$ the mean f at this R/R_e . This procedure effectively gives a minimum scatter in the stellar mass fraction that has formed at R/R_e or R/R_{BH} . Re-deriving the results that follow in terms of absolute physical radii (at fixed M_{tot}) we find the same qualitative results with systematically more scatter at all radii, for the reasons given above.

Figure 1 shows the results. We begin with a large sample of observed elliptical/spheroid surface brightness profiles from Kormendy et al. (2009) and Lauer et al. (2007), ~ 180 unique local ellipticals with nuclear *HST* observations and ground-based data at large radii (allowing accurate surface brightness profile measurements from ~ 10 pc to ~ 50 kpc). Conversion to stellar mass profiles and comparison of profiles from different instruments and wavebands are discussed extensively in Hopkins et al. (2008b, 2009a,d, 2008a, 2009c); for our purposes the results are identical. We consider the scatter in mass fraction enclosed $\sigma[M(< R)/M_{\text{tot}}]$ as a function of R/R_e in four bins of stellar mass, where there are sufficient numbers of observed objects (at least ~ 40 per bin) to obtain robust constraints.

There is a clear mass-independent trend of scatter with R/R_e , which we find can be reasonably well approximated as

$$\sigma[f(< R/R_e)] \approx -0.28 \log(R/R_e). \quad (3)$$

The scatter must go to zero, by definition, at $R = R_e$ because, by definition, all galaxies have exactly half their mass inside this radius, but the rise towards smaller radii reflects a physical diversity of profile shapes. Repeating this exercise in terms of physical radii in small mass bins, a nearly identical trend is recovered, with a systematically higher scatter at all radii by ~ 0.2 dex, and asymptoting to a constant ~ 0.2 dex scatter at radii corresponding to the typical R_e at that mass and larger.

Moreover, we have calibrated the expected results based on some simple experiments. For example, consider the case where we begin with a constant density profile over a number of fixed bins in R (analogous to the observed points) for some number of test cases, then independently perturb $\Sigma(R)$ with a lognormal fixed scatter (say ~ 0.3 dex) at each R , and using the new density profiles for each system reconstruct Figure 1. We recover the “appropriate” answer — namely, that while the scatter does go to zero as $R \rightarrow R_e$, the scatter at $R \ll R_e$ converges to the input lognormal scatter as the number of mock systems is increased.

Figure 1 shows that at $R \sim 0.1 R_e$, there is a factor 2 (0.3 dex) scatter in the interior stellar mass fraction, and that this grows to a factor ~ 4 (0.6 dex) at $R \sim 0.01 R_e$ and factor ~ 8 (0.8 dex) scatter near the BH radius of influence, $R \sim 0.001 R_e$. In other words, by the time one is inside just 10% of R_e , there is already more variation (galaxy-to-galaxy at fixed stellar mass) in the amount of mass that has “made it in” to smaller R than there is scatter in BH masses; this

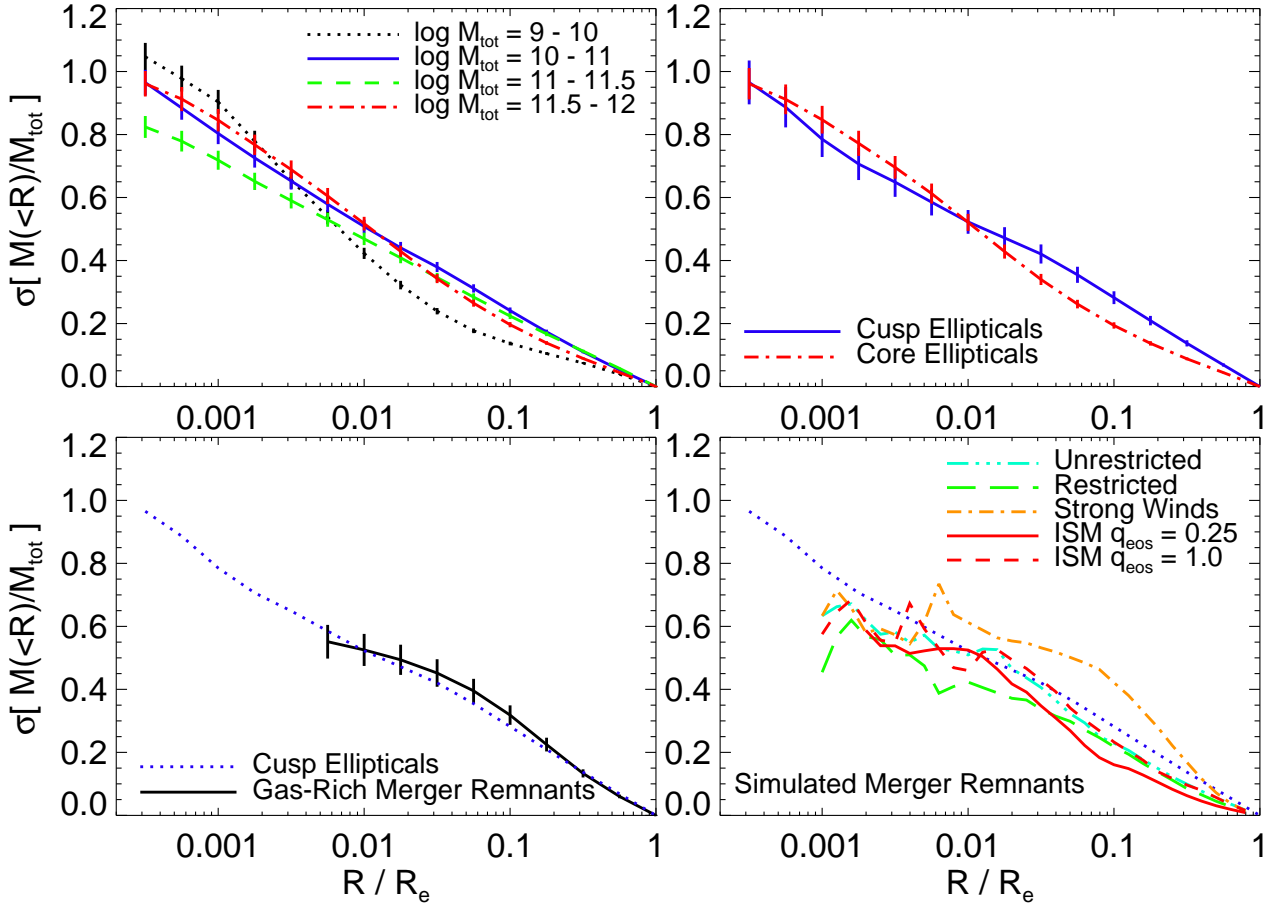


Figure 1. Top Left: Scatter in the enclosed stellar mass fraction versus R/R_e for ellipticals from the samples of Kormendy et al. (2009) and Lauer et al. (2007), in bins of stellar mass. Note $\sigma[M(<R)/M_{\text{tot}}] = 0$ at $R = R_e$, by definition. At small radii, the scatter increases significantly. Top Right: Same, but for the most well-studied mass range ($\sim L_*$), and with the sample divided into nuclear “cusp” and “core” galaxies. Although the median central profile shapes are different, $\sigma[M(<R)/M_{\text{tot}}]$ is relatively independent of cusp/core status, suggesting no more than weak dependence of σ on subsequent evolution and “scouring.” Bottom Left: The “cusp” result compared with mass profiles of observed recent gas-rich merger remnants (Rothberg & Joseph 2004). The profiles in scatter agree, suggesting that the diversity in stellar mass at small scales is put in place by the recent star formation in gas inflows. Bottom Right: Comparison between the “cusp” ellipticals and the relaxed remnants of a diverse set of *simulated* gas-rich mergers (see §3). In all cases, $\sigma[M(<R)/M_{\text{tot}}]$ increases at small radii.

difference only grows more and more pronounced as one moves to smaller radii.

It is perhaps possible that some of this diversity on small scales owes to evolution subsequent to the formation and growth of the BH itself. For example, the difference between ellipticals with central “cusps” and those with nuclear “cores” (steep versus flat central profile slopes, respectively) is commonly attributed to “scouring,” or the scattering of stars from an initially cuspy profile in three-body interactions by a binary BH after a “dry” or dissipationless galaxy merger (Begelman et al. 1980). To check this, we repeat our comparison in Figure 1 (upper right panel) separately for galaxies classified as “cusp” and “core” systems (classifications for each object are given along with surface brightness profiles). To obtain the most robust statistics, we consider a bin in total stellar mass near $\sim L_*$ ($M_{\text{tot}} = 10^{10} - 10^{11} M_\odot$), where our sample includes ~ 30 each of the cusp and core populations. At higher and lower masses, the comparison is similar, but the number of cusp and core ellipticals, respectively, drops rapidly. We find that there is no dramatic difference between the scatter within each of the two populations: the scatter in the amount of enclosed stellar mass increases dramatically at smaller radii for both cusp and core ellipticals.

Alternatively, we can compare the results for galaxies that

are known to be recent gas-rich merger remnants. Specifically, we repeat our analysis for the sample of confirmed gas-rich merger remnants with near-infrared surface brightness profiles from Rothberg & Joseph (2004), also discussed in the same context as the elliptical profiles above in Hopkins et al. (2008b). These objects are relatively young, so have not had much opportunity to be affected by subsequent evolution, although they are sufficiently evolved such that they are dynamically relaxed at $R \lesssim R_e$. As discussed in Hopkins et al. (2008b) we exclude all objects with obviously unrelaxed features such as e.g. shells or tidal tails inside these radii, and check that the dynamical times at the radii of interest are shorter than the mean stellar population/secondary burst population ages. Although the resolution for these objects does not reach the extremely small radii of the Virgo elliptical *HST* sample, the sample still overlaps over more than two orders of magnitude in R/R_e . The lower left panel of Figure 1 shows that the scatter derived from this sample agrees well with the trend seen in cusp ellipticals of the same mass. We have experimented both with the entire merger remnant sample taken together and that sample binned by mass, and we find that our conclusions and the quantitative and qualitative shape of the scatter are unchanged.

We emphasize that our discussion of the scatter in the enclosed

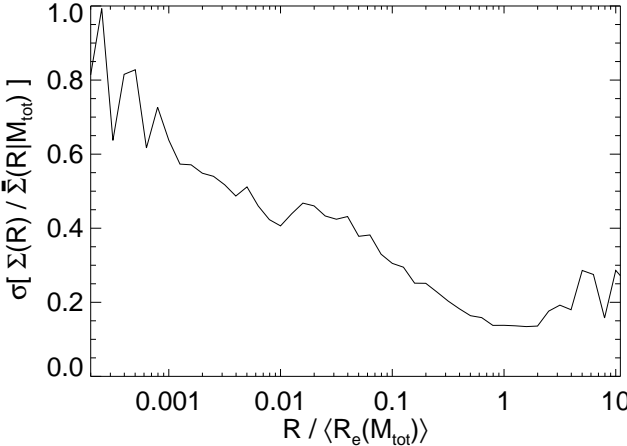


Figure 2. As Figure 1, but showing the logarithmic scatter in the stellar surface mass density $\Sigma(R)$ (equivalently, mass in some annulus at R) relative to some median profile shape for ellipticals of similar stellar mass ($\bar{\Sigma}(R|M_{\text{tot}})$), as a function of radius R relative to the effective radius of that median profile $\langle R_e(M_{\text{tot}}) \rangle$ (the median R_e of spheroids of the given mass). In a narrow stellar mass bin, this is equivalent to the scatter in $\Sigma(R)$ at each R . Dividing the sample as in Figure 1 yields similar results. The scatter does not vanish at $\langle R_e(M_{\text{tot}}) \rangle$, but it is small – this reflects the scatter in the size-mass relation. The rise in scatter to small radius is similar to Figure 1 – the trends reflect genuine increased scatter in central properties, not an artifact of the fitting/quantities plotted.

stellar mass with respect to the M_{BH} –host correlations implicitly assumes that all galaxies in the sample lie on the observationally established M_{BH} –host correlations, even though for many systems a BH mass has yet to be established. However we have examined the ~ 10 cases in the adopted samples that do have directly determined BH masses (compiled from Tremaine et al. 2002; Marconi & Hunt 2003; Häring & Rix 2004; Aller & Richstone 2007) and find that they are consistent with the above conclusions. The observed BH mass and radius of influence (calculated from the observed BH mass and velocity dispersion profile) agree with the simple estimates based on a constant BH to host mass ratio above. The scatter in e.g. the ratio $M_{\text{BH}}/M_{\text{gal}}(< R)$ exceeds an order of magnitude for $R \ll R_e$, as predicted in Figure 1. For $R \gtrsim R_e$ ($M(< R) \rightarrow M_{\text{tot}}$), on the other hand, the scatter in $M_{\text{BH}}/M_{\text{gal}}(< R)$ approaches the canonical ~ 0.3 dex. Bear in mind, however, that the number of such systems is small – rigorously re-fitting a BH-host mass relation as a function of mass in different radii and estimating the internal scatter will require larger overlapping samples with directly determined BH masses.

As noted above, the definition adopted implicitly guarantees the scatter vanishes at $R = R_e$. In the interests of looking for a location where the scatter is “minimized,” it is useful to define a similar quantity without this feature (even if the interpretation is somewhat less intuitive). For example, the scatter in surface stellar mass density relative to some median profile of galaxies at the same mass. We show this in Figure 2.

At a given stellar mass, we define the “median” profile as a de Vaucouleurs (1948) $r^{1/4}$ law with the same total stellar mass, but an effective radius equal to the median effective radius $\langle R_e \rangle$ of galaxies at that mass (from a quadratic fit to the $R_e - M_{\text{tot}}$ relation in the sample). Knowing this $\langle R_e(M_{\text{tot}}) \rangle$, the median profile is then

$$\bar{\Sigma}(R|M_{\text{tot}}) \equiv B_4 \frac{M_{\text{tot}}}{\langle R_e(M_{\text{tot}}) \rangle^2} \exp \left\{ -b_4 \left(\frac{R}{\langle R_e(M_{\text{tot}}) \rangle} \right)^{1/4} \right\} \quad (4)$$

where B_4 and b_4 are the appropriate normalization constants. We can then consider the ratio of the actual stellar mass surface density⁴ $\Sigma(R)$ to $\bar{\Sigma}(R|M_{\text{tot}})$. Figure 2 plots the logarithmic scatter in this ratio at fixed value of $R/\langle R_e(M_{\text{tot}}) \rangle$ (i.e. fixed R relative to the median R_e at a given mass): i.e. Equation 2 where $f = \Sigma(R)/\bar{\Sigma}(R|M_{\text{tot}})$ in some narrow interval (here 0.1 dex intervals) in $R/\langle R_e(M_{\text{tot}}) \rangle$. Because we are interested in the scatter, the median profile shape is implicitly normalized out; the results in Figure 2 are nearly unchanged if we assume a different Sersic profile with e.g. $n = 2 - 8$, or construct a non-parametric mean profile.

The results are similar to Figure 1: the scatter in surface density at a given radius (clearly related to the scatter in enclosed mass inside some radius) scales in a similar manner, reaching an order of magnitude at sufficiently small radii. Unlike Figure 1, the scatter does not have to go to zero at $R = R_e$; rather, at $R = \langle R_e(M_{\text{tot}}) \rangle$, the scatter reflects that in the size-mass relation of ellipticals (see e.g. Shen et al. 2003). Nevertheless, the scatter is much smaller around R_e (and may even reach a minimum at these radii – rising again at $R \gg R_e$, reflecting the diversity in outer profile shapes where e.g. the presence or absence of extended envelopes is important). Likewise, the conclusions are the same as Figure 1 if we split the sample by stellar mass or cusp/core status.

3 THEORY: THE SCATTER IN THE ENCLOSED STELLAR MASS FRACTION IN SIMULATIONS

We can gain some insight into how this scatter arises, and what it means relative to the amount of gas supply that has been available to the BH, by comparing with the results of numerical simulations of galaxy interactions and mergers that drive gas inflows, and that form realistic elliptical galaxies. Specifically, we consider the sample of hydrodynamic simulations in Cox et al. (2006), Robertson et al. (2006), and Younger et al. (2008) analyzed in detail in Hopkins et al. (2008b, 2009a,d, 2008a, 2009c,b). These amount to several hundred unique simulations, spanning a wide range in progenitor galaxy masses, gas fractions, orbital parameters, progenitor structural properties (sizes, concentrations, bulge-to-disk ratios), and redshift. Most of the simulations are major (mass ratios $\sim 1:3 - 1:1$), binary encounters, but they also include a series of minor mergers (from mass ratios $\sim 1:20$ to $\sim 1:3$), as well as spheroid-spheroid “re-mergers” or “dry mergers” (i.e. mergers of the elliptical remnants of previous merger simulations), mixed-morphology (spiral-elliptical) mergers (see also Burkert et al. 2008; Johansson et al. 2009), multiple mergers, and rapid series of hierarchical mergers. Our results presented below are robust to these choices in the simulations.

The numerical calculations usually include accretion and feedback from supermassive black holes, as well as feedback from supernovae and stellar winds. However, we have performed parameter studies in these feedback prescriptions, and find that the structural properties of interest here are relatively insensitive to these effects

⁴ We determine the stellar surface mass density profile for each object from its surface brightness profile by assuming a constant stellar mass-to-light ratio as a function of radius and normalizing to the total stellar mass. The stellar masses are determined from the multi-band photometry (integrated until the light is converged), using the color-dependent mass-to-light ratio calibrations in Bell et al. (2003), assuming a “dust” Salpeter (1955) IMF. Details are discussed in Hopkins et al. (2009a); changing the IMF, bands used, or allowing for a radius-dependent stellar mass-to-light ratio (based on the observed color gradients) makes little difference.

(Cox et al. 2009; Hopkins et al. 2007a, 2008b). These calculations broadly reproduce the mean and individual profile shapes of objects in the observed samples, as a function of stellar mass, age, morphology, and galaxy type, as well as the fundamental plane scaling relations of spheroids. Since this sample reproduces the median and scatter in profile shapes, we have some confidence that it represents a reasonable proxy for the amount of gas inflow in real ellipticals.

Figure 1 (bottom right panel) compares the scatter in interior mass fraction $\sigma[M(< R)/M_{\text{tot}}]$ for this sample of simulations with the result for observed cusp ellipticals (blue dotted line). We consider several sub-samples of simulations to see how this scatter depends on input parameters. First, we define an “unrestricted” sample that includes our entire suite of simulations. Second, we include a “restricted” sample that picks out a subset of nearly identical simulations. These simulations have galaxies with similar gas content at the time of the final merger, identical stellar masses, include only equal-mass mergers, and are chosen from a narrow range in orbital parameters. The scatter in this case comes, therefore, *only* from essentially random object-to-object variance in the exact dynamics of the merger, and consequently in the exact amount of gas that is stripped of angular momentum at various radii. That the scatter in the resulting stellar mass fraction is already almost as much as that in the “unrestricted” sample demonstrates that most of the scatter in the full sample is a consequence of the random processes in a merger, rather than a result of the initial differences in gas fraction or orbital parameters. Thus, it is difficult to marginalize the scatter by invoking, for example, a narrow distribution in these parameters at a given BH mass.

Third, we consider simulations with very strong stellar winds; these simulations are discussed in detail in Cox et al. (2009). They include a mass loading factor several times the star formation rate and high wind velocities — effectively representing the maximum wind feedback strength allowed by observations (see e.g. Martin 1999; Erb et al. 2006; Erb 2008). Cox et al. (2009) demonstrate that yet stronger winds yield results which are physically inconsistent with observations: galaxies “blow apart” any gas concentration so efficiently that the existence of a starburst becomes impossible. Thus, these “strong winds” simulations represent a reasonable physical upper limit to stellar feedback. The resulting dependence of scatter on radius is similar in the resulting galaxies, but with systematically higher normalization.

Finally, we consider a subset of simulations with two different specific choices for the sub-resolution prescription for the ISM gas (specifically the ISM equation of state: effectively the pressure support attributed to feedback loops in the ISM such as star formation, supernovae, stellar winds, radiation pressure, cosmic rays, and other sources; see e.g. McKee & Ostriker 1977; Springel & Hernquist 2003; Thompson et al. 2005). This is parameterized conveniently with the parameter q_{eos} : $q_{\text{eos}} = 0$ being an isothermal equation of state for the ISM, the situation most unstable to e.g. clumping and gravitational fragmentation, and $q_{\text{eos}} = 1$ representing the full Springel & Hernquist (2003) equation of state, which (over the density regime of interest) acts effectively as $P \propto \rho^{1.3-2.0}$, leading to an ISM more resistant to clumping and gravitational instability, with stronger pressure forces resisting infall and less stochastic scattering or torquing of gas clumps. Our results are similar in either case because the details of the gas physics or stellar feedback prescriptions are largely secondary with respect to gravitational torques, which dominate the dynamics in a merger (Hopkins et al. 2009b).

Given these comparisons, we can see how the scatter in stellar mass content — which the simulations accurately reproduce for

$R/R_e \gtrsim 0.001$ — relates to the scatter in the gas content “available” to fuel the BH. Figure 3 shows this comparison. Specifically, we compare the correlation between BH mass and host spheroid stellar mass from the simulations (see Di Matteo et al. 2005; Robertson et al. 2006), with a small lognormal scatter of ≈ 0.25 dex, to the correlation between a number of measures of the nuclear gas and the bulge mass. First (upper right-hand panel), we consider the maximum gas mass at any time during the merger that is available inside of a nominal small radius (here 100 pc; the results scale with radius in the manner seen in Figure 1; at smaller radii, however, our simulations begin to suffer from resolution limitations). We obtain a nearly identical result if we consider the *total* gas content that enters or is supplied to a given radius (and of course, the total gas content that ultimately stays in a given radius and is turned into stars is shown in Figure 1). The scatter is clearly much larger than that between BH mass and host bulge mass, specifically in this case 0.72 dex. Second, we consider the gas mass in this radius (“available” for accretion — i.e. having made it to less than 100 pc inside the center of the starburst/gas inflow) at the time of the peak accretion rate/intrinsic luminosity of the BH — i.e. just before feedback from the BH begins to regulate growth of the system. Here (lower left-hand panel), the scatter is even larger, almost a full order of magnitude (0.97 dex). Finally, in the lower right-hand panel, we consider the maximum gas mass inside 1% of the effective radius (or fixed multiple of the BH radius of influence), analogous to Figure 1.⁵ The scatter is similar to that in the fixed 100 pc radius, and to that expected from Figure 1, 0.69 dex.

Regardless of how we define the central gas content available for BH accretion, it seems that the scatter in the nuclear gas supply is always much larger than the scatter in BH mass at fixed host mass, in these simulations. Identical results are obtained in terms of other host properties like the velocity dispersion or binding energy.

It is interesting to compare these predictions to alternative, more extreme feedback models, in which the BH mass and resulting feedback set the total stellar mass itself by inducing star formation and/or blowing out all but some desired amount of gas, which will then (later) form stars. This contrasts strongly with the simulations above, where the BH forms in a largely fixed background potential of stars, and self-regulates its own growth (with the mass blown out by the BH being a small correction to the total bulge mass). In the models where the BH induces the bulge formation, the mass formed at some R is an explicit function of M_{BH} or BH luminosity: $M(< R)$ is a function of M_{BH} , rather than the other way around. As such, it is difficult to explain why the central regions of the galaxy near the BH radius of influence show a large scatter with respect to M_{BH} , while the mass formed at large radii, where the BH gravity is negligible, appears to reflect M_{BH} accurately. Quantitatively, we can construct analogous — albeit highly simplified — predictions for these models to compare with the standard self-regulated BH growth scenario simulated above. Specifically, we can repeat the calculations used to derive the expected BH-host mass relation in the models, allowing for some fluctuation in gas profile shapes. For example, we follow King (2003) and assume that BH feedback drives a compressive shock through a large gaseous body, inducing the formation of a bulge on the observed relation. Specifically, we assume that the gas initially follows a universal profile $\bar{\rho}(r)$ (in this case isothermal or Hernquist (1990), but it makes little difference for any $\rho \propto r^{-\beta}$ with $\beta < 3$, appropriate

⁵ Here, we consider the true three-dimensional effective radius of the system.

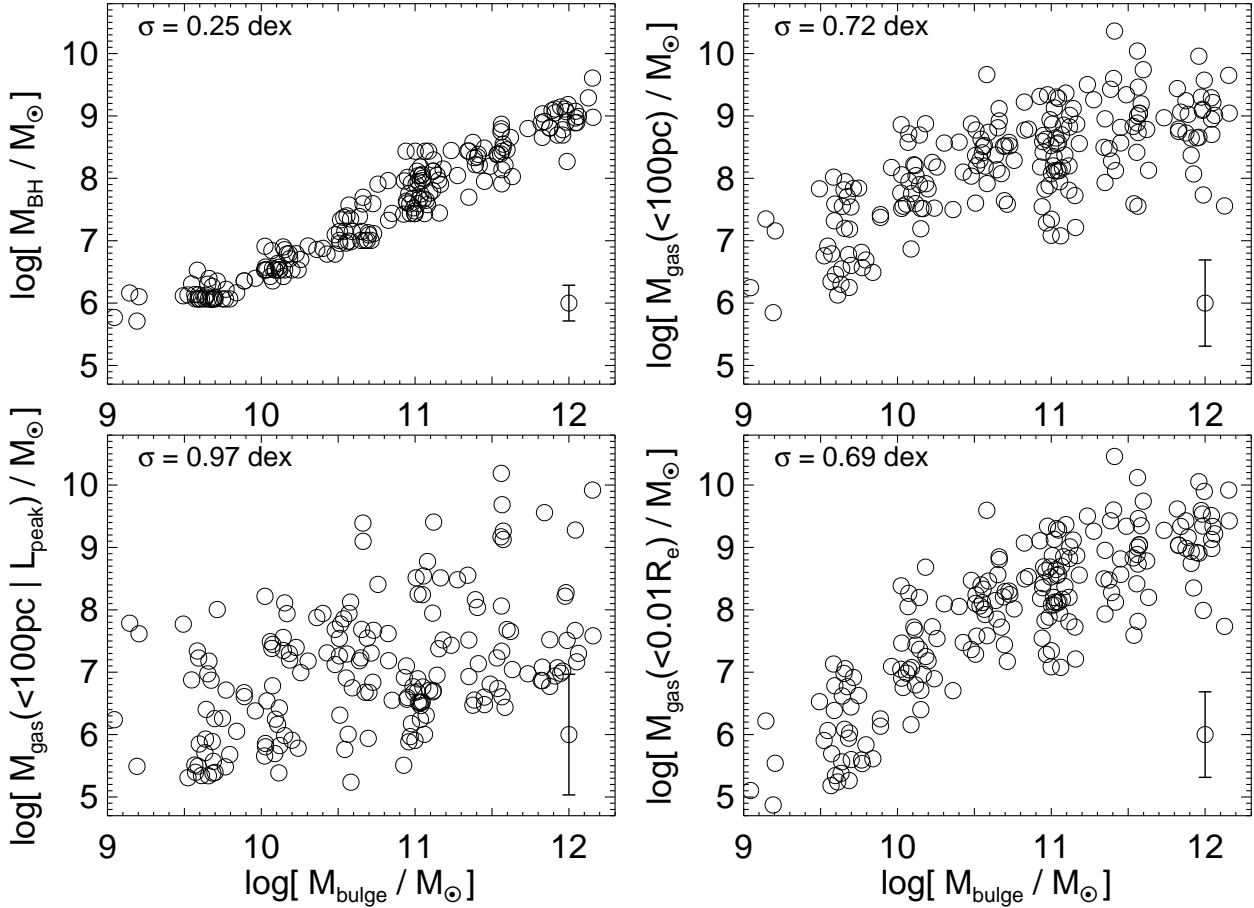


Figure 3. Results from simulated merger remnants. *Top Left:* BH mass versus host bulge mass. The intrinsic scatter is shown (0.25 dex). *Top Right:* Maximum gas mass (at any time during the merger) within 100 pc of the BH, as a function of host bulge mass. A similar result is obtained if we consider the total gas mass that at some point enters the central 100 pc, or the mass in stars in this radius, as shown in Figure 1. The intrinsic scatter is three times larger. *Bottom Left:* Same, but for the gas mass inside 100 pc at the time when the BH is growing at its peak rate. *Bottom Right:* Same, but for the maximum gas mass measured within a fixed fraction of the remnant effective radius, rather than at fixed physical radius. In these simulations, the BH mass is more sensitive to global quantities, such as the stellar mass, that set the local potential depth/escape velocity, rather than the local gas content.

for the radii $r < R_e$ that we are considering), and that the feedback drives a cold, infinitely thin shell which forms stars according to the observed Kennicutt (1998) relation; the details of the shell evolution are derived in King (2003, 2005). Now allow for some noise spectrum in object-to-object density profiles $\rho(r) = \bar{\rho}(r)(1 + \delta(r))$ ($\delta(r)$ is the amplitude of fluctuations in density per logarithmic interval in r , which we can parameterize⁶ as $\delta(r) \propto r^\gamma$) – this can represent clumping, fragmentation of shells, slightly different gas thermal states, inflow rates, or other factors. Integrating gives a prediction for the scatter in the log of the enclosed mass, as a function of radius: very approximately $\sigma[f(< R/R_e)] \propto \gamma + 0.5 \log R$. This is straightforward to understand: as the blastwave propagates away from the BH, the “knowledge” of the BH mass (accuracy with which the feedback strength at R reflects the true BH mass) ex-

cutes a random walk. It is, however, opposite the observed trend (Equation 3) for most reasonable input noise spectra. This clearly represents a strong constraint on these models. But it may be possible to reconcile them with the observations – for example, by invoking the observed trend as part of the initial conditions, imposing an initial spectrum of density perturbations that already resembles what is observed.⁷ This may be possible if, as demonstrated in the numerical simulations considered, gas is torqued and can move gravitationally in clumps and streams through an already largely formed stellar/dark matter background. However recall that in these models the background must (by construction) be primarily a self-gravitating gas-dominated system. It is unclear whether or not there actually exist equilibrium gas density profiles that can support (in an object-to-object sense) variations with as steep a spectrum as $\gamma \sim -1$ (for the observed scatter, this would imply that the same median equilibrium large-scale profile could support variations of

⁶ Equivalently, if there is some characteristic size scale $r_0 \propto r^\eta$ for fluctuations in ρ and the density is a local gaussian random field, then $\gamma = (1 - \eta)/2$. Equal magnitude of random density fluctuations/deviations per logarithmic interval in r corresponds to $\gamma = 0$ or $\eta = 1$ ($r_0 \propto r$). Constant physical size-scales for characteristic fluctuations give $\gamma = 1/2$. If the fluctuations seen in Figure 1 were put in as an initial condition in the density profile, it would be $\gamma = -0.3$ ($\eta = 1.6$).

⁷ In detail following the calculation above, the initial perturbation spectrum would have to be tuned as a function of radius such that $\gamma = -0.8$ ($\eta = 2.6$); the fractional amplitude of local density perturbations reflecting the location within the galaxy and characteristically about two orders of magnitude larger at ~ 100 pc than at the effective radius.

an order of magnitude in the density inside ~ 100 pc, for example). If not so, other radius-dependent sources of scatter would need to be invoked to reconcile these models and the observations.

4 CONCLUSIONS

We have compared the scatter in the stellar mass in the central regions of observed spheroids, as a proxy for the amount of gas which was available at a given radius for possible accretion by the central super-massive BH. The scatter in this proxy for gas supply, from galaxy to galaxy, at fixed stellar mass, increases rapidly at small radii. It is nearly an order of magnitude around the BH radius of influence. We show that this is true for both observed nuclear cusp and core ellipticals, and for observed recent gas-rich merger remnants (see Fig. 1; §2).

Despite this order-of-magnitude variation on small scales, the observed correlations between BH mass and global large-scale parameters of host spheroids (e.g., total stellar mass, velocity dispersion, binding energy) exhibit only factor ~ 2 scatter. In other words, the BH seems to “know more” about the host on large scales than on small scales. This is a natural expectation in feedback-regulated models: BHs stop growing once they reach a sufficient mass/accretion rate to unbind material near them, regardless of the total fuel supply. However, this finding is difficult to understand in the context of classes of models in the literature that do not invoke feedback and self-regulation, but instead posit that a fixed, small fraction, of the total host mass is incorporated into the central BH. If this were the case — if this gas supply set the BH mass — then the scatter in the nuclear gas supply would likely be directly related to the scatter in BH mass, and it should decrease or stay constant towards smaller radii. In fact, this is not observed.

As a check, and in order to provide context, we compare the observed scatter with hydrodynamic merger simulations that include feedback from growing BHs (see lower right-hand panel of Fig. 1, Fig. 3, and §3). We find that the observed trends are broadly reproduced by the simulations. At various points in a galaxy’s history, mergers and interactions efficiently remove angular momentum from the gas, such that some of the gas (at some initial radii) effectively free-falls until shocking near the galactic center. As a consequence, the scatter in the amount of gas that reaches a given small radius is set primarily by gravitational physics, rather than the details of the gas microphysics or feedback prescriptions. We demonstrate explicitly that the scatter is also a general result of even very similar initial conditions: at small radii, the chaotic nature of mergers and interactions is important, and even strong restrictions in the initial gas fractions, redshifts, and orbits of interacting systems does not significantly decrease the scatter in gas supply on scales comparable to the BH radius of influence. We also find that the simulations validate our assumption that the enclosed stellar mass is a faithful proxy for the supplied gas mass. Of course, it remains to be seen if this will be true as well for more “quiescent” fueling mechanisms (e.g. galactic bars and minor mergers, or stellar mass loss), that may be important or even dominant in the AGN population.

These findings relate to another interesting property of spheroids: the absolute value of the central/peak stellar surface density of spheroids is observed to be relatively constant (factor $\sim 3 - 5$ scatter) independent of e.g. total stellar mass or effective radius of the galaxy (see e.g. Lauer et al. 2007; Kormendy et al. 2009; Hopkins et al. 2009a), which vary widely. If BH mass were set purely by local processes, the simplest expectation from this fact

would be that all galaxies should correspondingly have the same BH mass (and that, as a consequence, there should be very large scatter between BH mass and *total* galaxy mass or velocity dispersion). Instead, it seems to be these integral properties, rather than local density, that correlate best with BH mass.

The constraints we derive on the run of observed scatter in stellar mass also appear constrain models at the opposite extreme. In these, feedback from the accreting BH is so strong that it determines the stellar mass of the galaxy, either by directly inducing star formation — essentially triggering bulge formation — or by blowing out a mass in gas much larger than the final stellar mass of the galaxy. In these models, galaxy mass is a function of BH mass, rather than the other way around. The scatter in the BH-host mass correlations is therefore a direct constraint on these models: in particular, not the absolute magnitude of the scatter, but the trend in scatter with radius is of interest. The stellar bulge mass formed in some shell at a given radius around the BH depends explicitly in these models on the BH mass (or luminosity), since this is what is triggering star formation or removing the gas supply that would otherwise make many more stars. Intuitively, it is difficult then to explain what is observed in Figure 1; despite the fact that the mass in each annulus should be determined by M_{BH} (if this class of models were true), the central regions of the galaxy show more scatter with respect to M_{BH} than the outer regions of the galaxy. In particular, the bulge mass at radii close to the BH radius of influence appears to have relatively little knowledge of the BH mass, exhibiting an order-of-magnitude scatter at given M_{BH} . In contrast, the mass formed at large radii, near the effective radius of the galaxy, here the BH’s gravity is completely negligible appears to trace the BH mass accurately. There may be particular initial conditions or other controlling parameters that explain this, but it is clear that the observed scatter can strongly constrain such models.

The systematics of the observed scatter in the BH-host relations therefore — perhaps moreso than the normalization or slope of the relations — suggests that BHs may indeed self-regulate at a critical mass determined by global host galaxy properties in the manner predicted by feedback models. At the very least, non-feedback models must be revisited. It is insufficient to predict the normalization and slopes of the BH-host correlations. They must also provide predictions that reproduce the small observed scatter at large radii and its significant increase at small radii. Likewise, models of very extreme feedback, in which the BH mass is not set by galaxy properties but rather, galaxy properties are set by BH mass, must explain how the central regions of the galaxy closest to the BH appear relatively insensitive to the BH mass. There is also the constraint from the BH “fundamental plane” — that it appears that neither $M_{\text{BH}} - \sigma$ nor $M_{\text{BH}} - M_{\text{bulge}}$ is most fundamental, but rather a combination that traces bulge binding energy ($\sim (M_{\text{bulge}} \sigma^2)^{0.7}$) (all models should predict, for example, that M_{BH} correlates with σ at fixed M_{bulge} and vice versa, as demonstrated in the observations in Hopkins et al. 2007b). Thus far, the class of self-regulating feedback models appear to be most successful at simultaneously explaining these observations, but more work is necessary.

Finally, we note that the simulations described in §3 indicate that the total stellar mass is a better predictor of M_{BH} than e.g. the stellar mass inside some small radius R . This prediction, coupled with the results in Figure 1, indicate that future observations of the galaxies that comprise the observed $M_{\text{BH}} - \text{host}$ relations should also consider the radius-dependence of those relations (i.e. $M_{\text{bulge}} - M_{\text{tot}}(< R)$ or $M_{\text{BH}} - \sigma(R)$ correlations, as a function of R). Comparison of such correlations, and identification of scales

where the scatter in the relations is minimized, can significantly constrain models of self-regulated BH growth.

ACKNOWLEDGMENTS

We thank Eliot Quataert, Carlos Frenk, and Lars Hernquist for helpful discussions. We also appreciate the hospitality of the Aspen Center for Physics, where this paper was partially developed. Support for PFH was provided by the Miller Institute for Basic Research in Science, University of California Berkeley.

REFERENCES

Aller, M. C., & Richstone, D. O. 2007, *ApJ*, 665, 120
 Arav, N., et al. 2007, *ApJ*, 658, 829
 Begelman, M. C., Blandford, R. D., & Rees, M. J. 1980, *Nature*, 287, 307
 Begelman, M. C., & Nath, B. B. 2005, *MNRAS*, 361, 1387
 Bell, E. F., McIntosh, D. H., Katz, N., & Weinberg, M. D. 2003, *ApJS*, 149, 289
 Burkert, A., Naab, T., Johansson, P. H., & Jesseit, R. 2008, *ApJ*, 685, 897
 Burkert, A., & Silk, J. 2001, *ApJL*, 554, L151
 Ciotti, L., & Ostriker, J. P. 1997, *ApJL*, 487, L105+
 —. 2001, *ApJ*, 551, 131
 Cox, T. J., Dutta, S. N., Di Matteo, T., Hernquist, L., Hopkins, P. F., Robertson, B., & Springel, V. 2006, *ApJ*, 650, 791
 Cox, T. J., et al. 2009, *ApJ*, in preparation
 Croton, D. J., et al. 2006, *MNRAS*, 365, 11
 de Vaucouleurs, G. 1948, *Annales d'Astrophysique*, 11, 247
 Di Matteo, T., Springel, V., & Hernquist, L. 2005, *Nature*, 433, 604
 Erb, D. K. 2008, *ApJ*, 674, 151
 Erb, D. K., Shapley, A. E., Pettini, M., Steidel, C. C., Reddy, N. A., & Adelberger, K. L. 2006, *ApJ*, 644, 813
 Escala, A. 2007, *ApJ*, 671, 1264
 Ferrarese, L., & Merritt, D. 2000, *ApJL*, 539, L9
 Gebhardt, K., et al. 2000, *ApJL*, 539, L13
 Graham, A. W., & Driver, S. P. 2007, *ApJ*, 655, 77
 Granato, G. L., De Zotti, G., Silva, L., Bressan, A., & Danese, L. 2004, *ApJ*, 600, 580
 Häring, N., & Rix, H.-W. 2004, *ApJL*, 604, L89
 Hernquist, L. 1990, *ApJ*, 356, 359
 Hopkins, P. F., Cox, T. J., Dutta, S. N., Hernquist, L., Kormendy, J., & Lauer, T. R. 2009a, *ApJS*, 181, 135
 Hopkins, P. F., Cox, T. J., & Hernquist, L. 2008a, *ApJ*, 689, 17
 Hopkins, P. F., Cox, T. J., Younger, J. D., & Hernquist, L. 2009b, *ApJ*, 691, 1168
 Hopkins, P. F., Hernquist, L., Cox, T. J., Di Matteo, T., Robertson, B., & Springel, V. 2006a, *ApJS*, 163, 1
 Hopkins, P. F., Hernquist, L., Cox, T. J., Dutta, S. N., & Rothberg, B. 2008b, *ApJ*, 679, 156
 Hopkins, P. F., Hernquist, L., Cox, T. J., Kereš, D., & Wuyts, S. 2009c, *ApJ*, 691, 1424
 Hopkins, P. F., Hernquist, L., Cox, T. J., Robertson, B., & Krause, E. 2007a, *ApJ*, 669, 45
 —. 2007b, *ApJ*, 669, 67
 Hopkins, P. F., Hernquist, L., Martini, P., Cox, T. J., Robertson, B., Di Matteo, T., & Springel, V. 2005, *ApJL*, 625, L71
 Hopkins, P. F., Lauer, T. R., Cox, T. J., Hernquist, L., & Kormendy, J. 2009d, *ApJS*, 181, 486
 Hopkins, P. F., Narayan, R., & Hernquist, L. 2006b, *ApJ*, 643, 641
 Hopkins, P. F., Robertson, B., Krause, E., Hernquist, L., & Cox, T. J. 2006c, *ApJ*, 652, 107
 Johansson, P. H., Naab, T., & Burkert, A. 2009, *ApJ*, 690, 802
 Kennicutt, Jr., R. C. 1998, *ApJ*, 498, 541
 King, A. 2003, *ApJL*, 596, L27
 —. 2005, *ApJL*, 635, L121
 Kormendy, J., Fisher, D. B., Cornell, M. E., & Bender, R. 2009, *ApJS*, 182, 216
 Lauer, T. R., et al. 2007, *ApJ*, 664, 226
 Li, Y., Haiman, Z., & Mac Low, M.-M. 2007, *ApJ*, 663, 61
 Magorrian, J., et al. 1998, *AJ*, 115, 2285
 Marconi, A., & Hunt, L. K. 2003, *ApJL*, 589, L21
 Martin, C. L. 1999, *ApJ*, 513, 156
 McKee, C. F., & Ostriker, J. P. 1977, *ApJ*, 218, 148
 Miralda-Escudé, J., & Kollmeier, J. A. 2005, *ApJ*, 619, 30
 Murray, N., Quataert, E., & Thompson, T. A. 2005, *ApJ*, 618, 569
 Nesvadba, N. P. H., Lehnert, M. D., Eisenhauer, F., Gilbert, A., Tecza, M., & Abuter, R. 2006, *ApJ*, 650, 693
 Peng, C. Y., Impey, C. D., Rix, H.-W., Kochanek, C. S., Keeton, C. R., Falco, E. E., Lehár, J., & McLeod, B. A. 2006, *ApJ*, 649, 616
 Prochaska, J. X., & Hennawi, J. F. 2009, *ApJ*, 690, 1558
 Reuland, M., et al. 2007, *AJ*, 133, 2607
 Robertson, B., Hernquist, L., Cox, T. J., Di Matteo, T., Hopkins, P. F., Martini, P., & Springel, V. 2006, *ApJ*, 641, 90
 Rothberg, B., & Joseph, R. D. 2004, *AJ*, 128, 2098
 Salpeter, E. E. 1955, *ApJ*, 121, 161
 Salviander, S., Shields, G. A., Gebhardt, K., & Bonning, E. W. 2007, *ApJ*, 662, 131
 Sazonov, S. Y., Ostriker, J. P., Ciotti, L., & Sunyaev, R. A. 2005, *MNRAS*, 358, 168
 Shen, S., Mo, H. J., White, S. D. M., Blanton, M. R., Kauffmann, G., Voges, W., Brinkmann, J., & Csabai, I. 2003, *MNRAS*, 343, 978
 Silk, J. 2005, *MNRAS*, 364, 1337
 Silk, J., & Rees, M. J. 1998, *A&A*, 331, L1
 Springel, V., Di Matteo, T., & Hernquist, L. 2005, *ApJL*, 620, L79
 Springel, V., & Hernquist, L. 2003, *MNRAS*, 339, 289
 Thompson, T. A., Quataert, E., & Murray, N. 2005, *ApJ*, 630, 167
 Tremaine, S., et al. 2002, *ApJ*, 574, 740
 Tremonti, C. A., Moustakas, J., & Diamond-Stanic, A. M. 2007, *ApJL*, 663, L77
 Woo, J.-H., Treu, T., Malkan, M. A., & Blandford, R. D. 2006, *ApJ*, 645, 900
 Wyithe, J. S. B., & Loeb, A. 2005, *ApJ*, 634, 910
 Younger, J. D., Hopkins, P. F., Cox, T. J., & Hernquist, L. 2008, *ApJ*, 686, 815